JACS
JOURNAL OF THE AMERICAN CHEMICAL SOCIETY
Communication
pubs.acs.org/JACS

Nanoscopic Cylindrical Dual Concentric and Lengthwise Block Brush Terpolymers as Covalent Preassembled High-Resolution and High-Sensitivity Negative-Tone Photoresist Materials

Guorong Sun,[†,‡,∥] Sangho Cho,[†,‡,∥] Corrie Clark,[†,‡] Stanislav V. Verkhoturov,[†] Michael J. Eller,[†] Ang Li,[†,‡] Adriana Pavía-Jiménez,[†,‡] Emile A. Schweikert,[†] James W. Thackeray,[*,§] Peter Trefonas,[*,§] and Karen L. Wooley[*,†,‡]

Departments of [†]Chemistry and [‡]Chemical Engineering, Texas A&M University, College Station, Texas 77842, United States
[§]Dow Electronic Materials, Marlborough, Massachusetts 01752, United States

Supporting Information

ABSTRACT: We describe a high-resolution, high-sensitivity negative-tone photoresist technique that relies on bottom-up preassembly of differential polymer components within cylindrical polymer brush architectures that are designed to align vertically on a substrate and allow for top-down single-molecule line-width imaging. By applying cylindrical diblock brush terpolymers (DBTs) with a high degree of control over the synthetic chemistry, we achieved large areas of vertical alignment of the polymers within thin films without the need for supramolecular assembly processes, as required for linear block copolymer lithography. The specially designed chemical compositions and tuned concentric and lengthwise dimensions of the DBTs enabled high-sensitivity electron-beam lithography of patterns with widths of only a few DBTs (sub-30 nm line-width resolution). The high sensitivity of the brush polymer resists further facilitated the generation of latent images without postexposure baking, providing a practical approach for controlling acid reaction/diffusion processes in photolithography.

Since chemically amplified lithographic techniques were established in the 1980s,[1] functional-polymer-based chemically amplified resists (CARs) have been investigated intensively to meet the simultaneous requirements of high sensitivity, high resolution, and low line-edge roughness (LER) for photolithography and other top-down lithographic techniques.[2] To date, varieties of CARs have been commercialized and extensively used to facilitate latent pattern features on a sub-30 nm scale.[2] As a new pathway to extend the size roadmap of microelectronic devices,[3] block copolymer lithography (BCL)[4] has emerged as a powerful bottom-up lithographic technique. BCL involves supramolecular assembly of block copolymers (BCPs) into periodic arrays of diverse morphologies within thin films on a scale of tens of nanometers.[5] To fabricate microelectronic circuitry, the BCPs are assembled into domains of differential composition, typically with cylindrical or lamellar morphologies, oriented perpendicular to the substrate surface.[5a,e,f,6] The morphology and orientation of BCP assemblies rely on the extent of immiscibility between the covalently bonded block segments and on the chemical compositions, block lengths, and block length ratio of the structural components,[4] requiring precise control to obtain large-scale vertical alignment of cylindrical assemblies.[5c−f,6]

Beyond linear polymers, there is increasing interest in exploiting polymers with nonlinear topologies as photoresist materials, such as Fréchet's dendritic polymers[7a] and Hadziioannou's hyperbranched polymers.[7b] In both cases, the branched architecture of the polymer framework constrains the chain entanglement and molecular size, thereby enhancing the overall patterning performance of the resist (i.e., higher sensitivity and lower LER) compared with their linear-polymer counterparts.

Inspired by these achievements, we developed a novel approach for photoresist polymer materials involving preconstruction of individually or collectively addressable block brush/graft terpolymer molecular brushes[8] that can align vertically on a substrate to form negative-tone molecular-scale resist features (Figure 1). The brush architecture was selected because it provides facile access to cylindrical nanoscopic objects[9] without the need for the supramolecular assembly processes that are typical with linear BCL. The diversity of chemical compositions and sizes can be tuned throughout the macromolecular brush framework with a high degree of control over the synthetic chemistry. The modularity of the bottom-up synthetic approach, based on sequentially "grafting through"[9] presynthesized polymer segments (macromonomers) with different compositions and functions for substrate alignment and cross-linking chemistry, respectively, into different regions of the molecular brush architecture, leads to efficient top-down patterning at the molecular level. As the current studies show, variation of the overall and relative lengths of the grafts versus the backbone allows the concentric and lengthwise dimensions to be modified conveniently, and control over the compositional placement within different regions of the cylindrical macromolecular framework provides a mechanism for aligning the polymer brushes and achieving electron-beam-generated patterns with widths of a few macromolecules.

As shown in Figure 1B, spin-casting deposition of a solution of the diblock brush terpolymer (DBT) and a photoacid generator (PAG) results in vertical alignment of the brushes on the

Received: December 27, 2012
Published: March 12, 2013

 © 2013 American Chemical Society

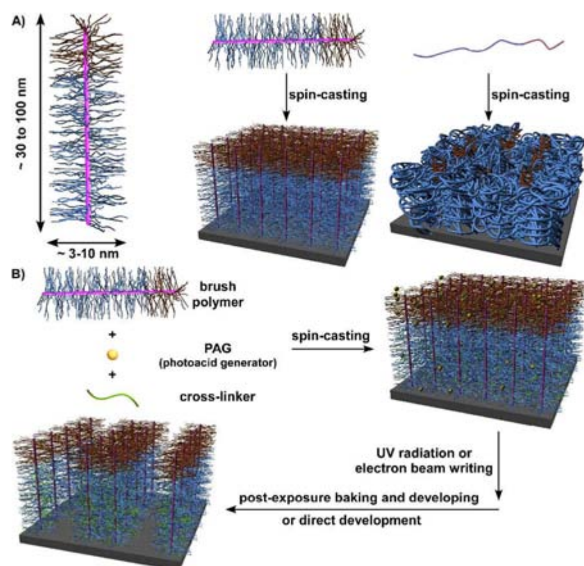

Figure 1. (A) Schematic representations of the targeted dimensions for the DBTs (left), their ideal alignment after deposition as a monolayer thin film (center), and for comparison, a linear BC thin film requiring multimolecular supramolecular assembly with morphological directionality (right). (B) Schematic diagram of the overall strategy.

substrate as a PAG-containing monolayer. UV or electron-beam irradiation through the predesigned pattern produces acid to promote cross-linking within the irradiated areas, with or without a postbaking step. Finally, solvent development reveals the latent patterned features. The target DBTs in this study were composed of densely grafted poly(tetrafluoro-*p*-hydroxystyrene) (PTF*p*HS) and poly(*p*-hydroxystyrene-*co*-*N*-phenylmaleimide) [P(*p*HS-*co*-PhMI)] side chains covalently tethered along a rigid polynorbornene (PNB) backbone in a block manner. The fluorinated P(NB-*g*-PTF*p*HS) segment acted as the vertical alignment promoter because of the relatively lower surface energy of fluoropolymers.[10] The phenol functionalities accommodated within the P(NB-*g*-P(*p*HS-*co*-PhMI)) structural segments provided attractive interactions with the substrate surface and also served as reactive sites for acid-catalyzed electrophilic aromatic substitution cross-linking chemistry.

The P(NB-*g*-PTF*p*HS)-*b*-P(NB-*g*-P(*p*HS-*co*-PhMI)) brushes were synthesized by applying sequential ring-opening metathesis polymerization (ROMP)[11] of NB-terminated macromonomers [NB−PTF*p*HS and NB−P(*p*HS-*co*-PhMI), respectively] (Scheme 1). Consequently, the construction of structurally well-defined NB−PTF*p*HS and NB−P(*p*HS-*co*-PhMI) macromonomers was critical for controlled block copolymerization during implementation of "grafting-through" ROMP. To date, direct controlled radical polymerization (CRP) of vinylphenol-based monomers remains a challenge, so protection and deprotection chemistries are frequently employed to obtain well-defined poly(vinylphenol) by CRP.[5d,6a] Herein we report a copolymerization method based on reversible addition−fragmentation chain transfer (RAFT),[12] the most versatile CRP methodology, to produce vinylphenol copolymers with well-defined structures, predictable and controllable molecular weights (MWs), and a norbornenyl α-chain terminus for use in the subsequent two-stage ROMP to afford the desired DBTs with variable dimensions.

Although the RAFT homopolymerization of TF*p*HS from a NB-terminated dithioester chain-transfer agent (CTA) pro-

Scheme 1. Synthesis of the Diblock Brush Terpolymers

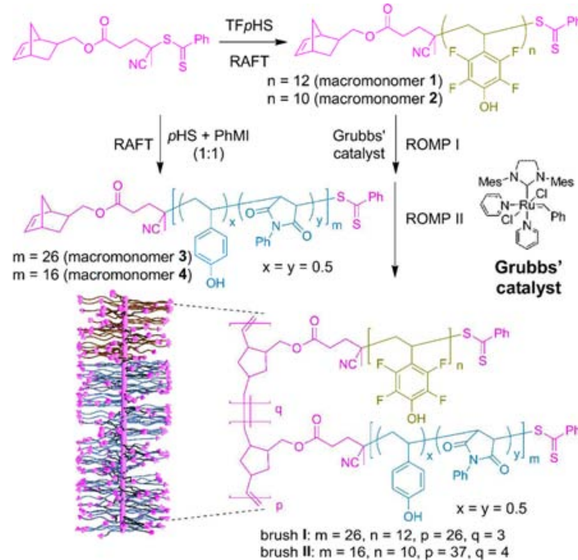

ceeded successfully to give macromonomers **1** and **2** [Scheme 1; see Figure S1 and Table S1, entries 1 and 2, in the Supporting Information (SI)], the RAFT homopolymerization of *p*HS (Table S1, entries 3 and 4) afforded polymers with broader MW distributions (Figure S2), indicating inadequate control. To obtain a macromonomer of *p*HS for use as the reactive majority of the molecular brush structure, we turned to RAFT copolymerization, as free-radical copolymerizations of *p*HS with methacrylates have recently been reported.[13] From the viewpoint of the comonomer pair, N-substituted maleimides were more effective candidates than methacrylates for RAFT copolymerization with *p*HS because of their well-documented low tendency to homopolymerize when undergoing significant cross-propagation with styrenic comonomers.[14] RAFT copolymerizations using *p*HS and PhMI as a comononer pair at a fixed 1:1 feed ratio afforded two macromonomers having different chain lengths (Table S1, entries 5 and 6). The well-defined structures of NB−P(*p*HS$_{13}$-*co*-PhMI$_{13}$) (**3**) and NB−P(*p*HS$_8$-*co*-PhMI$_8$) (**4**) (Scheme 1) were verified by ^{1}H NMR analysis (Figure S3B,C) through the ca. 1:1 integral ratio of the NB alkenyl protons (6.08 ppm) to the *m*-phenyl protons of the RAFT agent chain end (7.85 ppm). Gel-permeation chromatography (GPC) showed that both **3** and **4** had monomodal MW distributions with relatively low polydispersity indices (PDIs) of ca. 1.20 (Figure S3A). **1** was also utilized in this copolymerization method as a macro-RAFT CTA to afford the diblock terpolymer NB−PTF*p*HS$_{12}$-*b*-P(*p*HS$_{48}$-*co*-PhMI$_{48}$) (Figure S4), which served as the block-terpolymer linear control (**LC**) for the following lithographic studies.

Sequential ROMPs of **1** or **2** and **3** or **4** with the modified Grubbs' catalyst were then used to construct P(NB-*g*-PTF*p*HS)-*b*-P(NB-*g*-P(*p*HS-*co*-PhMI)) DBTs with variations in both the concentric and lengthwise dimensions (Scheme 1). The DBT P(NB-*g*-PTF*p*HS$_{12}$)$_3$-*b*-P(NB-*g*-P(*p*HS$_{13}$-*co*-PhMI$_{13}$))$_{26}$ (**I**) (M_n^{GPC} = 189 kDa, PDI = 1.25, 1.45 wt % F) was prepared at a [catalyst]:[**1**]:[**3**] feed ratio of 1:4:30. For the DBT [P(NB-*g*-PTF*p*HS$_{10}$)$_4$-*b*-P(NB-*g*-P(*p*HS$_8$-*co*-PhMI$_8$))$_{37}$ (**II**) (M_n^{GPC} = 152 kDa, PDI = 1.26, 2.00 wt % F), a 1:4.2:28 [catalyst]:[**2**]:[**4**] feed ratio was applied. The polymerizations were monitored by GPC, and obvious peak shifts were noticed during each ROMP process (Figure S5A,B). The ROMP I reaction efficiencies were

dx.doi.org/10.1021/ja3126382 | J. Am. Chem. Soc. 2013, 135, 4203−4206

estimated as 80% for **1** and 90% for **2** after 40 min. In ROMP II, both **3** and **4** showed >90% conversion after 180 min to afford **I** and **II** with narrow, monomodal MW distributions. The concentric block structures within **I** and **II** were verified by ^{1}H NMR spectroscopy and differential scanning calorimetry. Two sets of phenolic protons centered at 9.50 and 11.20 ppm (Figure S5C) and two glass transition temperatures at 130 and 150 °C were observed, corresponding to the P(*p*HS-*co*-PhMI) and PTF*p*HS grafts, respectively.

Polymer thin films were then prepared by spin-casting 1.0 wt % solutions of **I**, **II**, or **LC** in cyclohexanone onto silicon wafers (see the SI for details). As characterized by tapping-mode atomic force microscopy (AFM), the 25 nm thick **LC** film showed noticeable heterogeneity (Figure S6A). By comparison, the films of **I** and **II** exhibited sufficiently homogeneous surface topographies (Figure S6B,C) with root-mean-square roughnesses of <0.2 nm. The film thicknesses measured by AFM were 25 ± 1 for **I** and 30 ± 1 nm for **II**, in agreement with the estimated lengths of the extended brush backbones (23 and 30 nm, respectively). The surface topographical homogeneities and approximately monomolecular layer thicknesses of the brush films suggested that the brush polymer components within the films adopted orientations perpendicular to the wafer surface.[15]

The vertical alignments of the brushes across the wafer surface were confirmed by secondary-ion mass spectrometry (SIMS) fluorine depth profiles (Figure S7). The F species in brush **II** were predominantly located within the topmost layer of the film with a thickness of ca. 7 nm, and no F "signal" was detected at depths >13 nm.[16] The vertical alignments could be attributed to the intrinsically cylindrical topology of the DBTs induced by the strong size-exclusion effects between covalently tethered dense polymer grafts. Meanwhile, the fluorinated block segments in the DBTs would promote and assist the vertical alignment as a result of their preferential surface migration driven by their relatively lower surface energies. The extents of brush vertical alignment were quantified by X-ray photoelectron spectroscopy (XPS) (Figure S8) and C_{60} SIMS (Figure S9) through analyses of the relative surface F contents [i.e., the ratios between the measured and theoretical (100% vertical brush alignment) values; see the SI for details]. For both brushes, the XPS measurements showed that ca. 55% of the brushes within films adopted vertical alignments across the substrate surface without any special treatment (Table S2). SIMS showed that ca. 65% of the brushes preferred the expected vertical orientation, consistent with the XPS results. Solvent-assisted annealing (SAA) of the brush films using acetone significantly improved the extent of vertical alignment, as the surface F contents increased to become approximately equal to the theoretical values (Table S2). The enhancement in vertical alignment after SAA was also observed in the SIMS depth profile (Figure S10) and further increased the hydrophobicities of the film surfaces, as confirmed by the increased static water contact angles and decreased surface energies of the films (Table S3).

Finally, the lithographic behaviors of the molecular-brush-based resists were explored. Triphenylsulfonium perfluoro-1-butanesulfonate was used as the PAG, and *N*,*N*,*N*′,*N*′,*N*″,*N*″-hexakis(methoxymethyl)-1,3,5-triazine-2,4,6-triamine (HMMM) was selected as both the multivalent cross-linker and acid quencher. With a typical formulation for linear poly(vinylphenol)-based CARs [0.75:0.15:0.10 (w/w/w) brush:HMMM:PAG in cyclohexanone),[17] negative-tone post-exposure-baking electron-beam lithography (PEB-EBL) of the brush CARs (**CAR-I** and **CAR-II**) was performed (Figure 2).

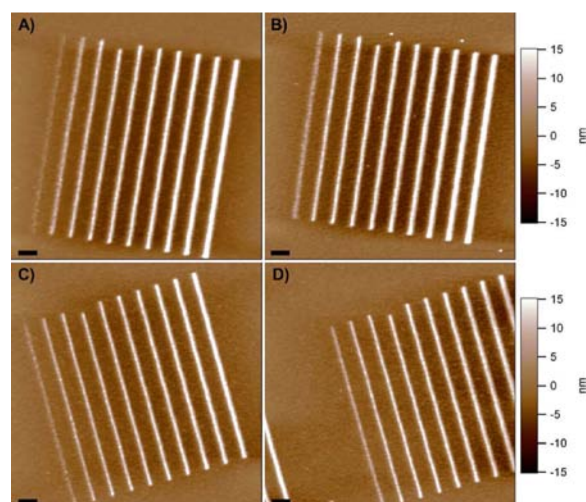

Figure 2. Tapping-mode AFM height images of PEB-EBL-generated patterns for (A, B) **CAR-I** and (C, D) **CAR-II** at exposure dosages of (A, C) 250 and (B, D) 400 μC/cm^2. Scale bars: 500 nm.

The lithographic performance was evaluated by AFM measurements of the heights and widths of lines in designed patterns with line widths of 10−100 nm at two exposure dosages (250 and 400 μC/cm^2). As opposed to the neat molecular brush materials, the static contact angles of the spin-cast and acetone-annealed resist films did not exhibit apparent differences (data not shown), which might be associated with migration of PAGs to the topmost layer of the resist films due to the F-enriched counterion in the PAG molecule. Therefore, the prepared resist films with thicknesses of 25 ± 2 nm (as measured by AFM) were directly used for lithographic studies.

Both **CAR-I** and **CAR-II** could be used to create patterns with full line integrities at each exposure dosage (Figure 2). In contrast, the patterns from **CAR-LC** had rational features only for 50−100 nm wide lines (Figure S11), even at 400 μC/cm^2. For the brush CARs in this study, the features of the latent 30−100 nm lines were satisfactory (Figure S12), especially for **CAR-II** at 400 μC/cm^2 (Figure 2D). We speculated that the better latent line-width features of **CAR-II** were induced by the intrinsic geometric factor of brush **II**, whose relatively shorter grafts make it a "thinner" column by reducing the chain entanglements after vertical alignment on the substrate surface. Under current instrumental conditions, a ca. 30 nm isolated line was obtained for **CAR-II** under the surveyed conditions. Thus, we can conclude that tuning of the lengthwise and concentric dimensions of the brush plays a critical role in the lithographic performance and that eventually molecular pixels could be realized through further systematic optimizations of the brush backbone and side-chain lengths and chemical compositions.

We also synthesized P(NB-*g*-P(*p*HS$_{13}$-*co*-PhMI$_{13}$))$_{24}$ as a brush control (**BC**) lacking the fluorocarbon-based block (Figure S13A) and subjected it to PEB-EBL under similar conditions. The resulting patterns did not exhibit the designed features (Figure S13B). Because of the lack of a fluorinated cap, **BC** adopted a random alignment across the wafer surface, and cross-linking occurred throughout the film because of the high sensitivity observed for brush CARs. These results further demonstrate the necessity of the combination of the brush architecture for high sensitivity and the block brush composition for vertical alignment and high-resolution imaging of brush polymers within the resist film.

Taking advantage of the higher sensitivity for the brush polymer CARs, we performed "direct" EBL (i.e., direct development of the electron-beam-exposed resists with no PEB) on **CAR-I** and **CAR-II** (see the SI for details). Interestingly, **CAR-II**, which showed better lithographic performance in PEB-EBL, could not generate latent patterns without PEB. In contrast, "direct" EBL of **CAR-I** was achieved for >50 nm wide features at an exposure dosage of 600 $\mu C/cm^2$ (Figure S14B), and the unexposed areas showed "cleaner" characteristics than the corresponding areas in PEB-EBL at an identical exposure dosage (Figure S14A vs Figure 2B).

In summary, diblock brush terpolymers with high degrees of versatility in chemical composition and concentric and length-wise dimensions were synthesized by RAFT polymerization/copolymerization to afford well-defined macromonomers followed by sequential ROMPs via the "grafting through" strategy. These cylindrical P(NB-*g*-PTF*p*HS)-*b*-P(NB-*g*-P(*p*HS-*co*-PhMI)) brushes exhibited a strong tendency to align vertically within thin films on substrates. The chemically amplified negative-tone PEB-EBL resists from the DBT precursors showed higher resolution and higher sensitivity than a linear block copolymer control. The thinner cylindrical DBTs could generate narrower line widths, whereas the thicker ones allowed "direct" EBL of brush CARs without a PEB step. Therefore, this bottom-up synthetic strategy enables fine-tuning of the full dimensions to balance the properties and performance during top-down lithographic processing. Further optimizations, including the introduction of aliphatic fluorinated caps to enhance the brush vertical alignment and the incorporation of covalently attached PAGs into molecular brush resist systems to achieve features with sub-10 nm resolution are currently underway.

■ ASSOCIATED CONTENT

Ⓢ Supporting Information

Experimental section and additional data. This material is available free of charge via the Internet at http://pubs.acs.org.

■ AUTHOR INFORMATION

Corresponding Author

jthackeray@dow.com; ptrefonas@dow.com; wooley@tamu.edu

Author Contributions

[‖]G.S. and S.C. contributed equally.

Notes

The authors declare no competing financial interest.

■ ACKNOWLEDGMENTS

The authors thank Dow Chemical Company (collaborative research agreement), the National Science Foundation (DMR-1105304), and the Welch Foundation (W. T. Doherty-Welch Chair, A-0001) for support, Dr. Phillip D. Hustad (Dow) and Dr. Jeffery E. Raymond (Texas A&M) for helpful discussions, and Ms. Rui Wang for help with illustrations.

■ REFERENCES

(1) (a) Fréchet, J. M. J.; Ito, H.; Willson, C. G. *Microcircuit Eng. 82 [Proc. Microcircuit Eng. Conf.]* **1982**, 260. (b) Fréchet, J. M. J.; Eichler, E.; Ito, H.; Willson, C. G. *Polymer* **1983**, *24*, 995.

(2) (a) Ito, H. *Adv. Polym. Sci.* **2005**, *172*, 37. (b) Grigorescu, A. E.; Hagen, C. W. *Nanotechnology* **2009**, *20*, No. 292001. (c) Sanders, D. P. *Chem. Rev.* **2010**, *110*, 321. (d) Prabhu, V. M.; Kang, S.; VanderHart, D. L.; Satija, S. K.; Lin, E. K.; Wu, W.-l. *Adv. Mater.* **2011**, *23*, 388. (e) Orski, S. V.; Fries, K. H.; Sontag, S. K.; Locklin, J. *J. Mater. Chem.* **2011**, *21*, 14135.

(3) International Technology Roadmap for Semiconductors. Overall Roadmap Technology Characteristics (ORTC) Tables, 2011; http://www.itrs.net/reports.html.

(4) (a) Bang, J.; Jeong, U.; Ryu, D. Y.; Russell, T. P.; Hawker, C. J. *Adv. Mater.* **2009**, *21*, 4769. (b) Kim, H.-C.; Park, S.-M.; Hinsberg, W. D. *Chem. Rev.* **2010**, *110*, 146.

(5) (a) Chai, J.; Wang, D.; Fan, X.; Buriak, J. M. *Nat. Nanotechnol.* **2007**, *2*, 500. (b) Bita, I.; Yang, J. K. W.; Jung, Y. S.; Ross, C. A.; Thomas, E. L.; Berggren, K. K. *Science* **2008**, *321*, 939. (c) Ruiz, R.; Kang, H.; Detchevery, F. A.; Dobisz, E.; Kercher, D. S.; Albrecht, T. R.; de Pablo, J. J.; Nealey, P. F. *Science* **2008**, *321*, 936. (d) Tang, C.; Lennon, E. M.; Fredrickson, G. H.; Kramer, E. J.; Hawker, C. J. *Science* **2008**, *322*, 429. (e) Park, S.; Lee, D. H.; Xu, J.; Kim, B.; Hong, S. W.; Jeong, U.; Xu, T.; Russell, T. P. *Science* **2009**, *323*, 1030. (f) Bates, C. M.; Seshimo, T.; Maher, M. J.; Durand, W. J.; Cushen, J. D.; Dean, L. M.; Blachut, G.; Ellison, C. J.; Willson, C. G. *Science* **2012**, *338*, 775.

(6) (a) Bosworth, J. K.; Black, C. T.; Ober, C. K. *ACS Nano* **2009**, *3*, 1761. (b) Park, S.-M.; Liang, X.; Harteneck, B. D.; Pick, T. E.; Hiroshiba, N.; Wu, Y.; Helms, B. A.; Olynick, D. L. *ACS Nano* **2011**, *5*, 8523. (c) Albert, J. N. L.; Bogart, T. D.; Lewis, R. L.; Beers, K. L.; Fasolka, M. J.; Hutchison, J. B.; Vogt, B. D.; Epps, T. H. *Nano Lett.* **2011**, *11*, 1351. (d) Jung, H.; Hwang, D.; Kim, E.; Kim, B.-J.; Lee, W. B.; Poelma, J. E.; Kim, J.; Hawker, C. J.; Huh, J.; Ryu, D. Y.; Bang, J. *ACS Nano* **2011**, *5*, 6164. (e) Tang, C.; Wu, W.; Smilgies, D.-M.; Matyjaszewski, K.; Kowalewski, T. *J. Am. Chem. Soc.* **2011**, *133*, 11802.

(7) (a) Tully, D. C.; Trimble, A. R.; Fréchet, J. M. J. *Adv. Mater.* **2000**, *12*, 1118. (b) Chochos, C. L.; Ismailova, E.; Brochon, C.; Leclerc, N.; Tiron, R.; Sourd, C.; Bandelier, P.; Foucher, J.; Ridaoui, H.; Dirani, A.; Soppera, O.; Perret, D.; Brault, C.; Serra, C. A.; Hadziioannou, G. *Adv. Mater.* **2009**, *21*, 1121.

(8) Sheiko, S. S.; Sumerlin, B. S.; Matyjaszewski, K. *Prog. Polym. Sci.* **2008**, *33*, 759.

(9) (a) Xia, Y.; Olsen, B. D.; Kornfield, J. A.; Grubbs, R. H. *J. Am. Chem. Soc.* **2009**, *131*, 18525. (b) Hosono, N.; Kajitani, T.; Fukushima, T.; Ito, K.; Sasaki, S.; Takata, M.; Aida, T. *Science* **2010**, *330*, 808. (c) Müller, M.; Yuan, J. Y.; Weiss, S.; Walther, A.; Fortsch, M.; Drechsler, M.; Müller, A. H. E. *J. Am. Chem. Soc.* **2010**, *132*, 16587. (d) Li, Z.; Ma, J.; Lee, N. S.; Wooley, K. L. *J. Am. Chem. Soc.* **2011**, *133*, 1228. (e) Johnson, J. A.; Lu, Y. Y.; Burts, A. O.; Lim, Y. H.; Finn, M. G.; Koberstein, J. T.; Turro, N. J.; Tirrell, D. A.; Grubbs, R. H. *J. Am. Chem. Soc.* **2011**, *133*, 559.

(10) Voet, V. S. D.; Pick, T. E.; Park, S.-M.; Moritz, M.; Hammack, A. T.; Urban, J. J.; Ogletree, D. F.; Olynick, D. L.; Helms, B. A. *J. Am. Chem. Soc.* **2011**, *133*, 2812.

(11) Sutthasupa, S.; Shiotsuki, M.; Sanda, F. *Polym. J.* **2010**, *42*, 905.

(12) Boyer, C.; Bulmus, V.; Davis, T. P.; Ladmiral, V.; Liu, J.; Perrier, S. *Chem. Rev.* **2009**, *109*, 5402.

(13) Gonsalves, K. E.; Wang, M.; Lee, C.-T.; Yueh, W.; Tapia-Tapis, M.; Batina, N.; Henderson, C. L. *J. Mater. Chem.* **2009**, *19*, 2797.

(14) (a) Pfeifer, S.; Lutz, J.-F. *J. Am. Chem. Soc.* **2007**, *129*, 9542. (b) Satoh, K.; Matsuda, M.; Nagai, K.; Kamigaito, M. *J. Am. Chem. Soc.* **2010**, *132*, 10003.

(15) (a) Paik, M. Y.; Xu, Y.; Rastogi, A.; Tanaka, M.; Yi, Y.; Ober, C. K. *Nano Lett.* **2010**, *10*, 3873. (b) Jeon, H.; Schmidt, R.; Barton, J. E.; Hwang, D. J.; Gamble, L. J.; Castner, D. G.; Grigoropoulos, C. P.; Healy, K. E. *J. Am. Chem. Soc.* **2011**, *133*, 6138.

(16) These depths were calculated from the full width at half-maximum of the F^-/CH_2^- intensity ratio.

(17) Lee, S. M.; Fréchet, J. M. J.; Willson, C. G. *Macromolecules* **1994**, *27*, 5154.

dx.doi.org/10.1021/ja3126382 | *J. Am. Chem. Soc.* 2013, 135, 4203−4206